PAPER • **OPEN ACCESS**

Micropattern-mediated apical guidance accelerates epithelial cell migration to improve healing around percutaneous gastrostomy tubes

To cite this article: Tyler J D'Ovidio *et al* 2019 *Biomed. Phys. Eng. Express* **5** 065027

Biomedical Physics & Engineering Express

PAPER

Micropattern-mediated apical guidance accelerates epithelial cell migration to improve healing around percutaneous gastrostomy tubes

Tyler J D'Ovidio[1], **Aidan R W Friederich**[2], **Nic de Herrera**[2], **Duncan Davis-Hall**[1,3], **Ethan E Mann**[2] and **Chelsea M Magin**[1,3,4]

[1] Division of Pulmonary Sciences and Critical Care Medicine, Department of Medicine, University of Colorado Anschutz Medical Campus, Aurora, CO, United States of America
[2] Sharklet Technologies, Inc., Aurora, CO, United States of America
[3] Department of Bioengineering, University of Colorado Anschutz Medical Campus, Aurora, CO, United States of America
[4] Author to whom any correspondence should be addressed.

E-mail: tyler.dovidio@cuanschutz.edu, aidanfriederich@gmail.com, ndeherrera@sharklet.com, duncan.davis-hall@cuanschutz.edu, emann@sharklet.com and chelsea.magin@cuanschutz.edu

Keywords: cell migration, micropattern, microtopography, wound-healing, percutaneous endoscopic gastrostomy, *in vitro* model

OPEN ACCESS

RECEIVED
5 July 2019

REVISED
15 October 2019

ACCEPTED FOR PUBLICATION
24 October 2019

PUBLISHED
6 November 2019

Abstract

Hypergranulation, bacterial infection, and device dislodgment are common complications associated with percutaneous gastronomy (PG) tube placement for enteral feeding largely attributable to delayed stoma tract maturation around the device. Stoma tract maturation is a wound-healing process that requires collective and complete migration of an advancing epithelial layer. While it is widely accepted that micropatterned surfaces enhance cell migration when cells are cultured directly on the substrate, few studies have investigated the influence of apical contact guidance from micropatterned surfaces on cell migration, as occurs during stoma tract formation. Here, we developed 2D and 3D *in vitro* epithelial cell migration assays to test the effect of various Sharklet micropatterns on apically-guided cell migration. The 2D modified scratch wound assay identified a Sharklet micropattern (+10SK50×50) that enhanced apical cell migration by 4-fold ($p = 0.0105$) compared to smooth controls over the course of seven days. The best-performing micropattern was then applied to cylindrical prototypes with the same outer diameter as a pediatric PG tube. These prototypes were evaluated in the novel 3D migration assay where magnetic levitation aggregated cells around prototypes to create an artificial stoma. Results indicated a 50% increase ($p < 0.0001$) in cell migration after seven days along Sharklet-micropatterned prototypes compared to smooth controls. The Sharklet micropattern enhanced apically-guided epithelial cell migration in both 2D and 3D *in vitro* assays. These data suggest that the incorporation of a Sharklet micropattern onto the surface of a PG tube may accelerate cell migration via apical contact, improve stoma tract maturation, and reduce skin-associated complications.

Background

Percutaneous endoscopic gastrostomy (PEG) feeding, introduced into clinical practice in the pediatric population in 1980 [1], is now established as an effective way to provide enteral feeding to patients who have functional gastrointestinal tracts but are unable to swallow for longer than four to six weeks [2]. Today, US hospitals utilize over 70,000 pediatric percutaneous gastrostomy (PG) tubes per year, leading to successful feeding in approximately 96% of patients [3]. Despite this high level of success, the device remains especially susceptible to complications immediately following PG tube placement. The PEG procedure uses endoscopic guidance to place a silicone tube directly into the stomach through a small incision through the abdominal wall [2]. Over the next two to four weeks the tract around the PG tube epithelializes forming a gastrocutaneous fistula called a stoma [4, 5]. One study of 221 pediatric patients revealed that over

70% experienced minor complications, with the most frequently encountered complications directly related to stoma formation, including hypergranulation, bacterial infection, skin breakdown, and device dislodgment [3, 6]. PG tube design improvements, including the replacement of external catheters with a skin-level button [7], have reduced the rate of complications over the years. However, stoma site complications remain a concern for tube placement in children and thus it is still a priority to expedite stoma tract maturation in order to prevent early complications after PG tube placement.

Stoma tract creation can be classified as a wound healing process that requires collective and complete migration of an advancing epithelial layer to achieve full maturation. During wound healing, a number of complementary directional signals drive epithelial cells, including both gradients of soluble biochemical cues and physical guidance from the surrounding extracellular microenvironment [8, 9]. In particular, the dermal-epidermal junction where epithelial cell migration occurs along human skin is not flat but is comprised of a series of microscale ridges and projections [10]. Studies by our group [11] and others [12–14] have demonstrated that micropatterns can replicate the physical contact guidance cues encountered by cells *in vivo* to enhance and direct the migration of both individual epithelial cells and of epithelial cells from the adjacent wound edges. Microgrooves ranging from 1 to 50 μm in width with heights of 0.6 to 150 μm have been shown to enhance and direct migration of epithelial cells *in vitro* [13–15]. The Sharklet micropattern, in particular, was deliberately designed to systematically influence cellular morphology [16] and migration [11, 17] when culturing cells on the micropatterned structure. While this micropattern orientation provides ideal healing application for a wound dressing integrated into the regenerated tissue [11], it does not recapitulate the same cell-device interactions that occur upon PG tube placement. In this scenario, the PG tube initially comes into contact with the apical surface of an existent cell layer that must rearrange in order to migrate along or incorporate into the surface of the implanted device [18]. The ability to guide cell migration through interaction with the apical cell surface has been investigated in only one two-dimensional (2D) study. Interestingly, Marmaras *et al* demonstrated that parallel microgrooves with a width of 2 μm and spacing of 1 μm enhanced wound coverage through apical application to a modified scratch wound assay created using human dermal fibroblasts compared to smooth surfaces [19].

Therefore, we hypothesized that applying the Sharklet micropattern, with feature heights ranging from 3 to 10 μm and spacing ranging from 2 to 50 μm, to the surface of silicone PG tube prototypes would improve epithelial cell migration rates and could potentially expedite stoma maturation, resulting in reduced risk of stoma-related complications. Here, we introduce a new assay for evaluating cellular migration in three-dimensions (3D) around cylindrical PG tube prototypes and investigate the potential for engineered micropatterns applied apically to enhance wound healing *in vitro*.

Methods

Sample fabrication

Smooth and micropatterned samples for 2D assays were manufactured by casting biomedical grade polydimethylsiloxane elastomer (silicone, Elastosil® M 4641 silicone; Wacker Chemie AG) against negative silicon wafer molds (figure 1(a)). Discontinuous channel features arranged in a Sharklet™ (SK) pattern with protruding (+) features with varied height, width, and spacing comprised these micropatterns. The following example defines shorthand nomenclature for the SK micropattern: a pattern with a height of 3 μm, a width of 10 μm, and spacing of 5 μm would be listed as +3SK10×5. Smooth controls (SM) and +3SK2×2, +3SK10×5, and +10SK50×50 micropatterns were fabricated for two-dimensional (2D) migration assays. Smooth and micropatterned cylindrical prototypes (diameter = 5 mm, length = 7 mm) were manufactured by injecting silicone (Elastosil® M 4641 silicone; Wacker Chemie AG) into a cylindrical mold and curing for one hour at 65°C (figure 1(b)). Samples were evaluated for pattern transfer and fidelity using confocal microscopy to acquire images (figures 1(c)–(f)) for analysis (Olympus LEXT OLS 4000). Feature height, width and spacing were measured and plotted (figures 1(g)–(i)). Smooth and +10SK50×50, the best-performing micropattern identified in 2D migration assays, prototypes were fabricated for testing in 3D assays.

2D apical wound healing assay

First, neonatal human epidermal keratinocytes (HEKn, Life Technologies, Carlsbad, CA) were labelled with a cytoplasmic dye according to the manufacturer's instructions, i.e., by incubating adherent cells with serum-free growth media containing 18 μm CellTracker Orange for 45 min (Cell Tracker Orange CMTMR [(5-(and-6)-((((4-chloromethyl)benzoyl)amino) tetramethylrhodamine], Life Technologies, Carlsbad, CA). A coating matrix kit consisting of human collagen I in solution (Life Technologies, Carlsbad, CA) was applied to the surface of 6-well tissue-culture plates for 30 min at room temperature. Next, placing SM silicone rectangles (3 mm × 34 mm) along the center of each well blocked cell attachment and created a modified scratch-wound assay [19–21]. Labelled-HEKns were then seeded onto the coated and blocked 6-well plates at 10,000 cells cm^{-2}. A defined growth medium (Cascade EpiLife medium containing 1% EDGS, 1% Pen Strep, and 0.5 $\mu g\ ml^{-1}$ amphotericin B maintained these cells at 37 °C and 5% CO_2.

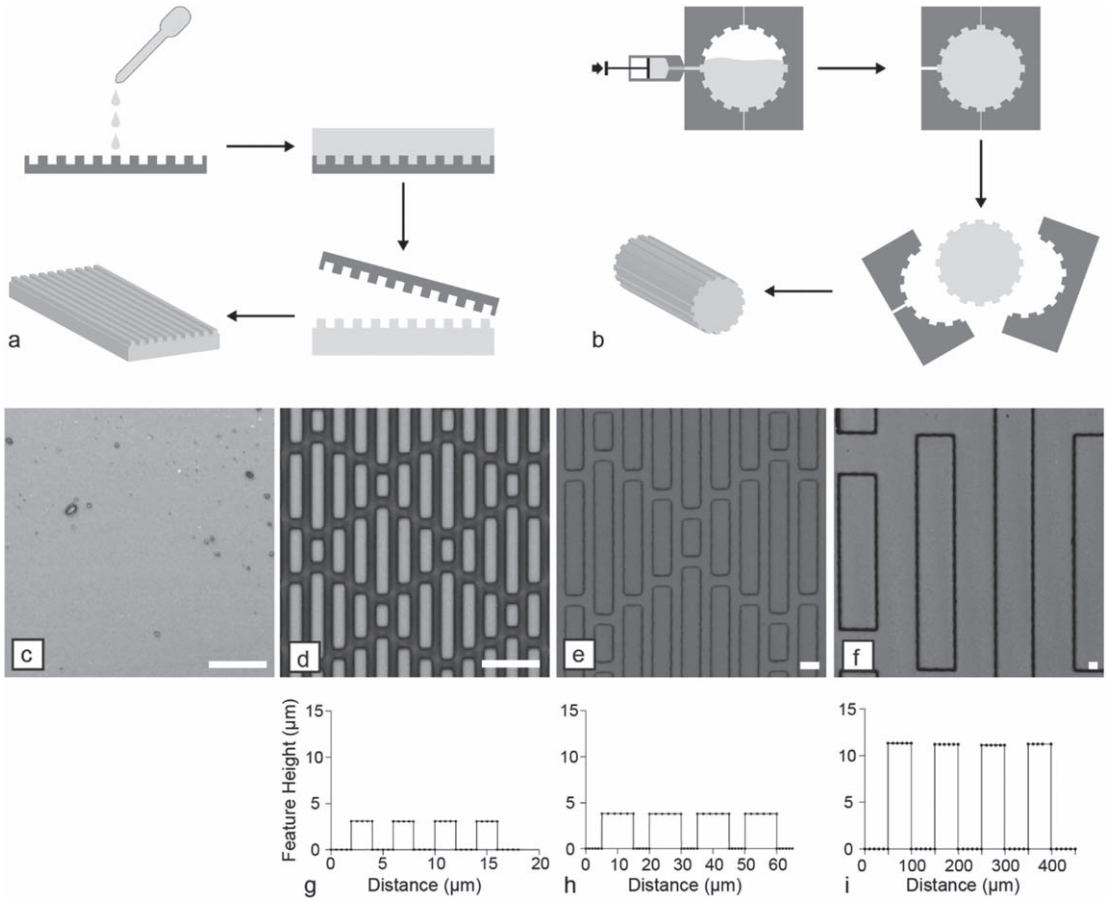

Figure 1. Schematic of the process for patterning biomedical-grade silicone (a) patches via silicon molds and (b) PEG tube prototypes via book molding. Representative confocal microscopy images of (c) SM, (d) +3SK2×2, (e) +3SK10×5 and (f) +10SK50×50 micropatterns replicated in biomedical grade silicone. Feature height, width and spacing measurements of (g) +3SK2×2, (h) +3SK10×5 and (i) +10SK50×50 micropatterns. Scale bars, 10 μm.

Once HEKns reached ~70% confluence, lifting the silicone rectangle generated an artificial wounded area. A SM or micropatterned silicone patch was immediately placed across the wound site (perpendicular to length of wound) (figure 2(a)). After one, three and seven days, samples were fixed with 4% paraformaldehyde (Electron Microscopy Sciences, Hatfield, PA) for 15 min at room temperature and then imaged using fluorescent microscopy.

Migration was quantified by measuring the area covered by cells within the artificial wound using ImageJ Software (National Institutes of Health [NIH], Bethesda, MD) [11]. The average area covered by cells was divided by the total artificial wound area for each sample [11] and this wound coverage value was normalized to that for each sample type on Day 1.

Cell shape analysis

Immunofluorescent images of CellTracker-labeled cells were processed and quantified using NIH ImageJ software. The software approximated each cell as an ellipse and measured the short and long axes of each ellipse. Cell alignment was measured by calculating the angle between the direction of the micropattern features and the long axis of each cell. Aspect ratio was calculated by dividing the length of the long axis by the length of the short axis for each cell.

3D wound healing assay

Smooth or micropatterned silicone prototypes were fixed to the center of a 24-well cell-repellent plate using biomedical grade silicone adhesive (SILASTIC™ Medical Adhesive Silicone, Type A, Dow Silicones Corporation) such that the length of the prototype ran parallel to the well walls. The adhesive cured for 2 h at room temperature. During this time, HEKns were labelled with a cytoplasmic dye (CellTracker Orange CMTMR, Life Technologies, Carlsbad, CA) by incubating cells with growth media containing 18 μM CellTracker Orange for 45 min. Next, HEKns were lifted from the surface of cell culture flasks using trypsin/EDTA (0.025% in phosphate buffered saline (PBS), Life Technologies), then rinsed with PBS to remove residual trypsin and loaded with NanoShuttle (Greiner Bio-One, Monroe, NC), a poly-L-lysine coated magnetic nanoparticle. Magnetic nanoparticles were added to cells at a concentration of 1 μl NanoShuttle per 1×10^4 cells. This mixture was centrifuged (100 xg for 5 min) and resuspended three times total prior to seeding. Magnetized HEKns were

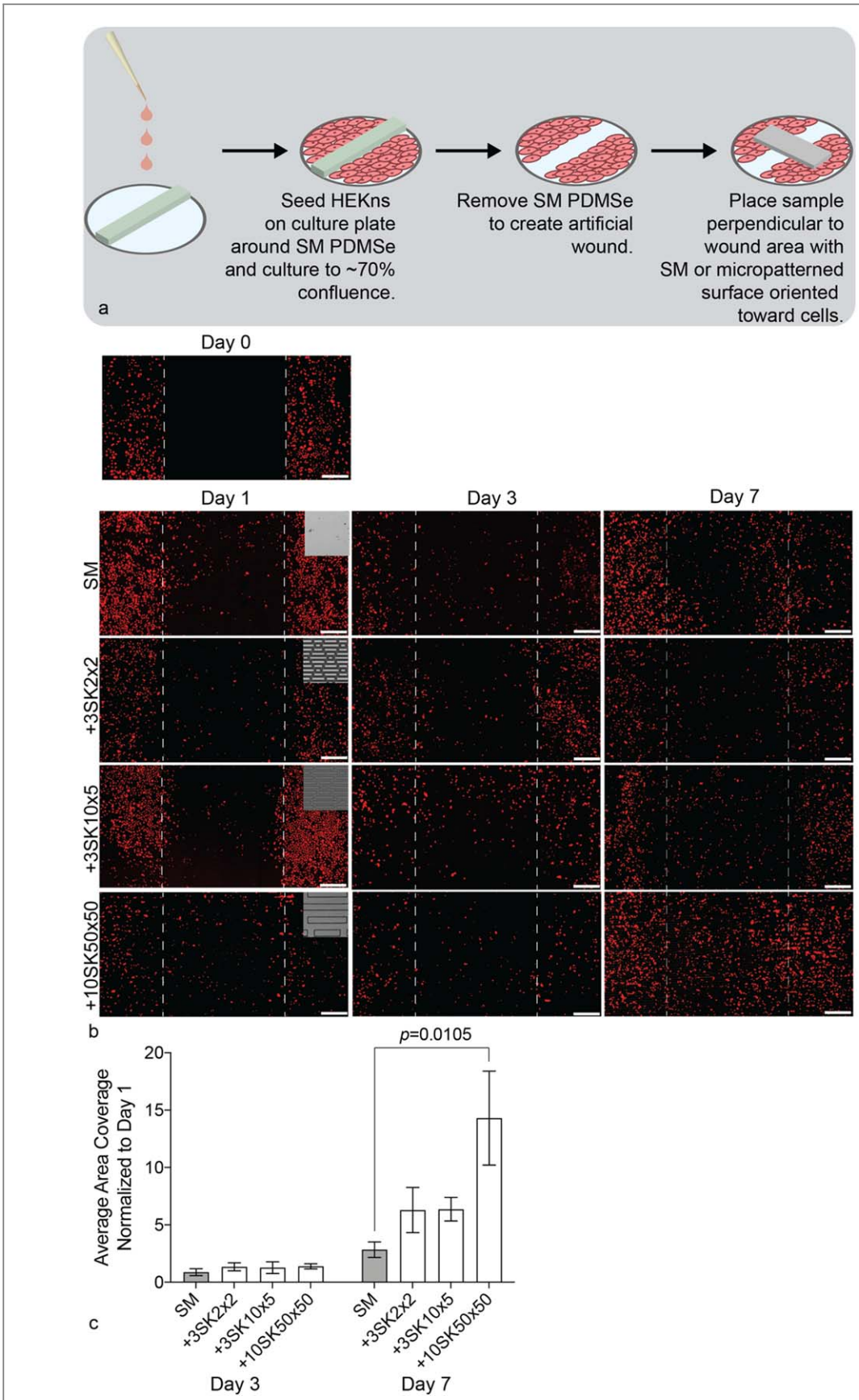

Figure 2. The +10SK50×50 micropattern increased apical HEKn migration significantly compared to SM controls. (a) Schematic depicting the 2D migration assay, including artificial wound area generation. (b) Representative fluorescent images of 2D HEKn (red) apical migration immediately after artificial wound generation (Day 0) and after 1, 3, and 7 days under micropatterned patches. Scale bar, 0.5 mm. (c) Quantification of migration within the wounded area demonstrates statistical improvement of apical migration under +10SK50×50 micropatterned wound patch compared to SM control at Day 7 ($N = 3$; $p = 0.0105$; Two-way ANOVA, Tukey Test).

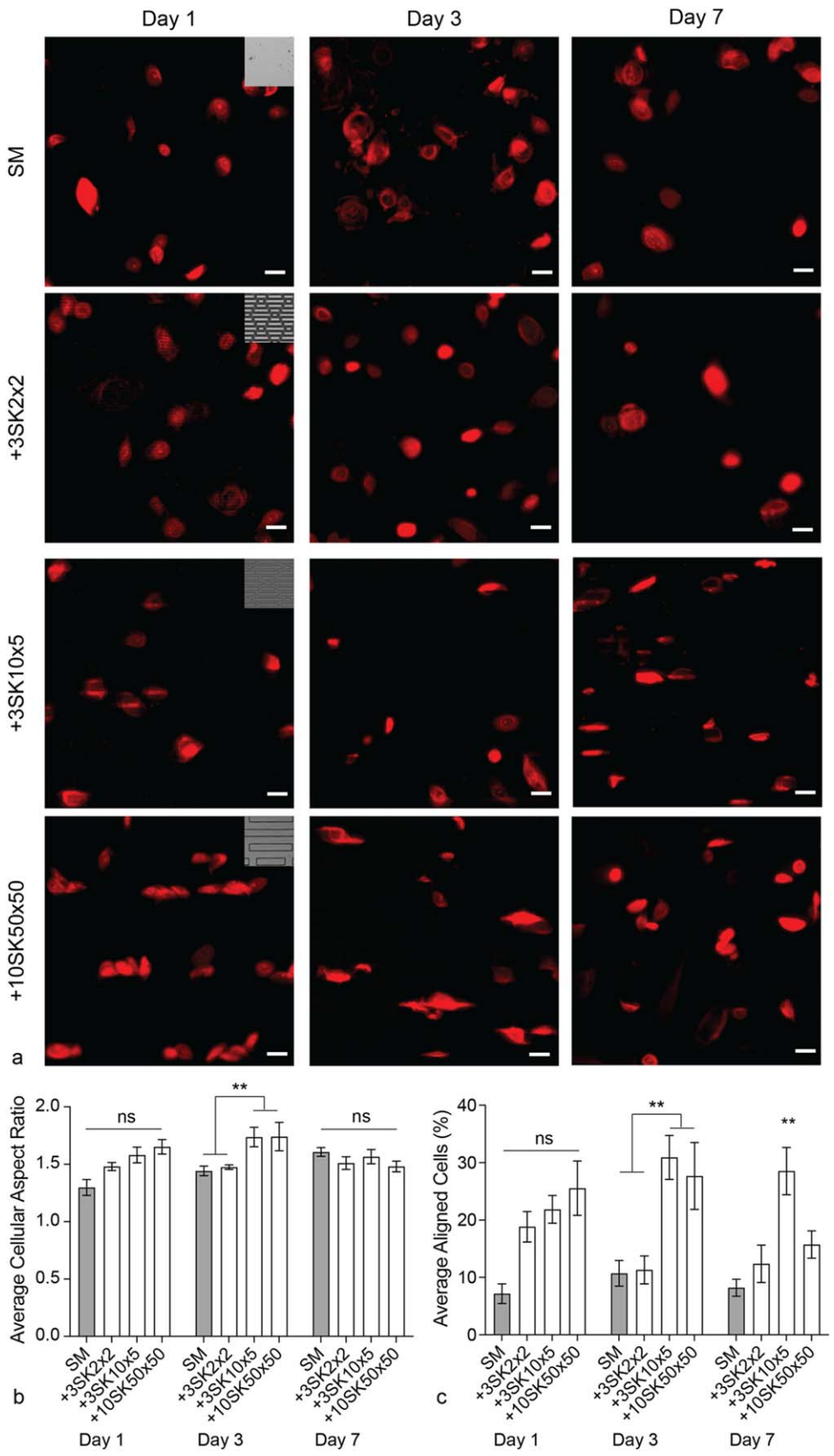

Figure 3. Micropatterns influence both cell shape and alignment when placed in contact with the apical cell surface. (a) Representative fluorescence microscopy images of HEKns (red) cultured under micropatterned surfaces at Days 1, 3 and 7. (b) Average cellular aspect ratio calculations show that two micropatterns significantly increased cellular elongation compared to SM controls at Day 3. (c) The percent of cells aligned within 10 degrees of the long axis of the micropattern features shows that micropatterns increase cellular alignment compared to SM at Day 3 and 7 ($^{**}p < 0.005$; ANOVA, Tukey Test).

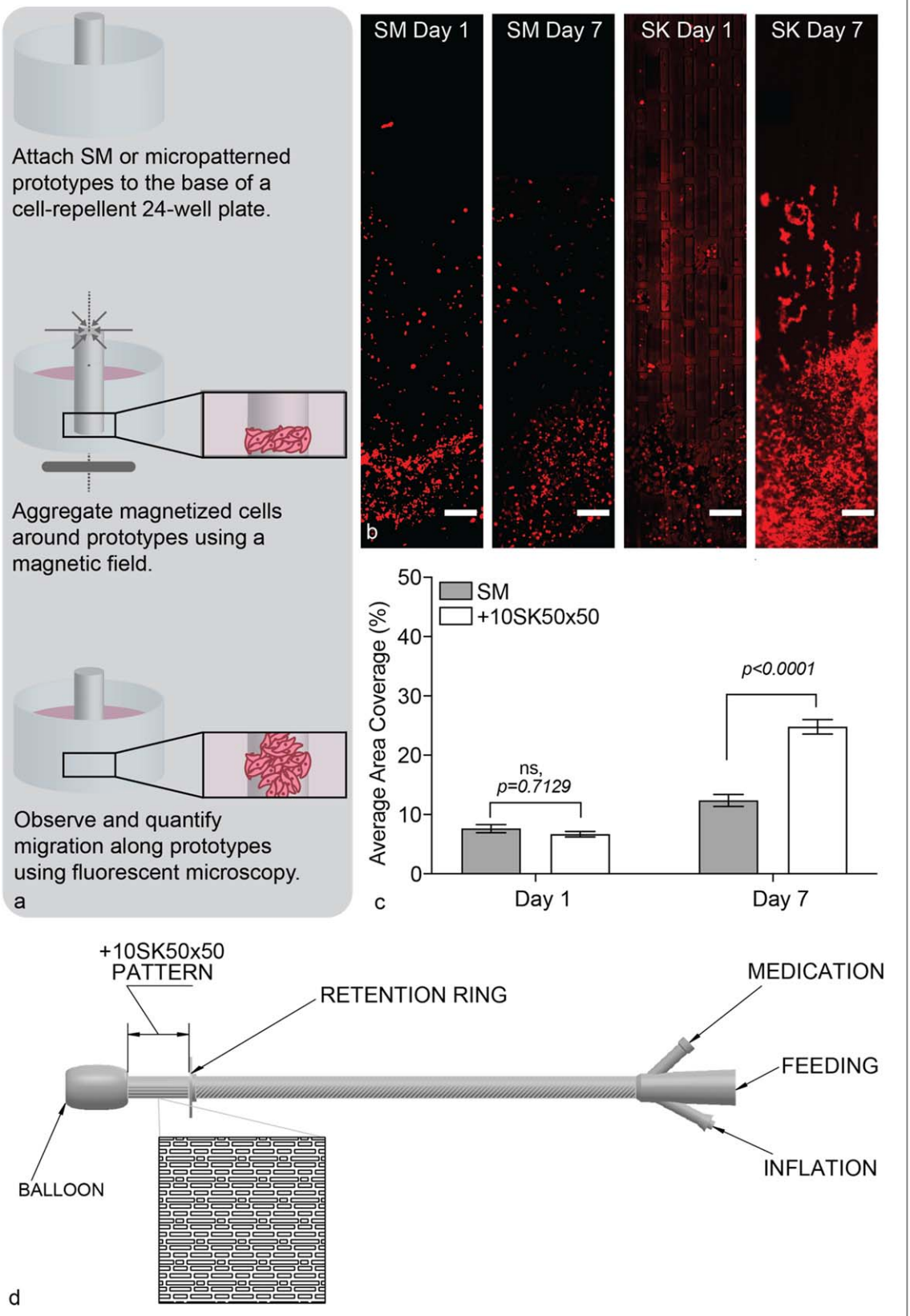

Figure 4. The + 10SK50×50 micropattern significantly increased cell migration on prototypes. (a) Schematic depicting experimental setup used to emulate stoma formation and quantify migration on micropatterned-prototypes in 3D. (b) Representative fluorescent images of 3D migration results from Day 1 and Day 7 time points on SM and +10SK50×50 micropatterned samples showing HEKns (red). Scale bar, 500 μm. (c) Quantification of migration using average area coverage along each prototype demonstrates there is no statistical difference between cellular aggregation on Day 1 and there is statistical improvement of migration on +10SK50×50 micropatterned samples compared to SM controls (3 biological replicates, n = 3 per biological replicate). (d) A drawing representing the portion of a PG tube that should be micropatterned in order to improve wound healing.

then seeded at 1×10^6 cells ml^{-1} (350 μl per well) in cell-repellent 24-well plates containing prototypes. Cells were magnetically levitated by applying a 24-Well Bio-Assembler (Greiner Bio-One, Monroe, NC) to the 24-well plate for 15 min at 37 °C and 5% CO_2 to form a pseudo stoma along the center of SM or micropatterned prototypes. The magnetic field was removed and cells were maintained in growth medium for 7 days (figure 4(a)). At the assay endpoint, 4% paraformaldehyde (Electron Microscopy Sciences, Hatfield, PA) fixed the cells for 15 min and imaged the prototypes via fluorescent microscopy (figure 4(b)). Migration was quantified by measuring the area covered by cells along three full-length images of each sample. ImageJ Software (National Institutes of Health [NIH], Bethesda, MD) calculated the average percent area coverage for each sample type at the assay endpoint (day seven) [11]. Experiments were performed in biological triplicates with $n = 3$ technical replicates.

Results

2D wound healing assay

Fluorescent imaging of artificial wound sites demonstrated consistent, identifiable wound areas following wound-patch removal (figure 2(b), Day 0). Imaging performed at Days 1, 3, and 7 of migration visualized progressive migration of HEKns into wounded space over the full course of experimentation (figure 2(b)). Quantification of Day 3 and Day 7 images normalized to Day 1 revealed no statistical differences between sample types at Day 3. The +3SK2×2 and +3SK10×5 micropatterns did not significantly enhance HEKn migration across the artificially generated wound area compared to SM controls on Day 7. The +10SK50×50 micropattern demonstrated statistically significant improvement in HEKn migration after 7 days, resulting in a 4-fold increase in wound area coverage compared to the SM control (figure 2(c), $p = 0.0105$; Two-way ANOVA, Tukey Test). Based on these results, the +10SK50×50 micropattern was chosen to be incorporated into prototypes for 3D apical wound healing assays.

Cell shape analysis

To track and measure cell morphology, HEKns were labeled with a fluorescent membrane dye (CellTracker Orange CMTMR, Life Technologies, Carlsbad, CA). Image analysis showed that the cellular aspect ratio increased as the aspect ratio of the micropattern features increased on Days 1 and 3 with statistically significant increases when cells were in contact with the +3SK10×5 and +10SK50×50 micropatterns on Day 3 ($^{**}p < 0.005$; ANOVA, Tukey Test). This trend was not observed at the Day 7 time point where no significant differences in cellular aspect ratio were measured. Likewise, the percentage of cells that were aligned within 10 degrees of the micropatterned features increased with increasing micropattern aspect ratio on Days 1 and 3 with statistically significant increases for cells treated with the +3SK10×5 and +10SK50×50 micropatterns on Day 3 ($^{**}p < 0.005$; ANOVA, Tukey Test). A significant increase in cellular alignment persisted on only the +3SK10×5 micropattern on Day 7 ($^{**}p < 0.005$; ANOVA, Tukey Test).

3D wound healing assay

Prototypes containing the +10SK50×50 micropattern significantly improved HEKn migration in a novel 3D wound healing assay designed to emulate stoma formation *in vitro* (figure 4(b)). Results demonstrated no statistical difference between the average area covered by cells upon aggregation around prototypes on Day 1 ($p = 0.7129$; ANOVA, Tukey Test). At the assay endpoint, Day 7, results revealed a statistically significant increase in average area coverage on the +10SK50×50 micropatterned prototypes compared to SM controls ($p < 0.0001$; ANOVA, Tukey Test) (figure 4(c)). These results confirm that the Sharklet micropattern accelerates HEKn migration around cylindrical samples that approximate the size and shape of standard pediatric PG tubes.

Discussion

Enteral nutritional support remains essential for management of pediatric patients with poor voluntary oral intake. Endoscopic methods in particular facilitate a variety of enteral feeding access options that improve patient outcomes and decrease costs. Despite the benefits and widespread use of PG tube feeding, many patients experience complications that range in severity and often require further clinical intervention [22]. Complications frequently occur within the first 30 days following PG tube placement while the maturing stomal tract remains particularly vulnerable to inadvertent removal or loosening [23]. Suboptimal stoma formation or widening of the stomal tract leads to leakage, increased risk of infection, skin breakdown, and accidental dislodgement [3]. Complete displacement of the PG tube prior to stomal tract maturation presents a serious complication that can require revision surgery and often results in secondary ailments associated with significant morbidity and mortality, including peritonitis and hemorrhage [24, 25]. While device designs, such as low-profile PG tubes, have evolved to address a variety of complications, device displacement remains a concern [26].

Accelerating this wound-healing process potentially promises to reduce device-related complications during stomal tract maturation. Stoma formation primarily occurs through migration of cells from the wound margins, identified as a rate-limiting step in the completion of wound closure [27]. Previous studies by our group [11] and others have shown that

micropatterned surfaces accelerate the migration step of wound healing [12, 14, 19] by directing the placement and maturation of focal adhesion complexes on device surfaces to guide cellular polarization and migration [28]. This mechanism has been validated in a variety of applications where the basal side of cells would attach directly to a wound dressing or other medical device [11–13]. The insertion of a PG tube, however, exposes the apical cell surface to the medical device, resulting in the need for an alternative approach to investigate the influence of micropatterns on stoma formation. One study by Marmaras *et al* evaluated this complementary mechanism for influencing cellular migration using micropatterns. This study paved the way for continued examination of apical cell migration by demonstrating that gratings with groove and ridge widths of 1 μm and depths of 0.6 μm applied to the apical surface of cells enhanced cell polarization, migration, and wound closure without the establishment of focal adhesions between cells and the test surface *in vitro* [19].

The results presented in the present study demonstrate that Sharklet micropatterns accelerate migration through apical application and highlight the development of a novel 3D assay that enabled the testing of PG tube prototypes approximating the size and geometry of the final device design. In 2D apical wound healing assays, the +10SK50×50 Sharklet micropattern, which comprises the largest feature heights, widths, and spacings, produced the highest increase in cell migration (4-fold increase, $p = 0.0105$) compared to smooth controls (figure 2(c)). PG tube prototypes subsequently integrated this micropattern for further evaluation. All micropatterns tested influenced cellular shape and alignment in 2D with significant increases in both measured after three days in culture (figure 3).

Recently, magnetic levitation has emerged as an advanced cell-culture technique that facilitates the aggregation of cells into 3D structures that better recapitulate native cellular microenvironments. A variety of different cell types bound to magnetic nanoparticles have levitated within an external magnetic field [29] to produce an array of enabling technologies including cell spheroids for toxicity testing [30], complex tissue structures such as heart valve leaflets for tissue engineering [31], and co-culture models of breast cancer tumor tissue [32]. Here, we implemented this technology for the first time to aggregate HEKn cells around PG tube prototypes to investigate cellular migration along the external surface of this medical device. The results from this model, developed specifically to recapitulate stoma formation, demonstrated a 50%, $p < 0.0001$ increase in cell coverage due to migration over seven days on Sharklet-micropatterned prototypes compared to smooth controls (figure 4(c)). This outcome indicates that Sharklet-micropatterned prototypes accelerate epithelial cell migration following initial contact with a pseudo-stoma *in vitro*. A fully mature stoma maintains a consistent, robust elasticity around the PG tube that minimizes leakage of gastric contents and the entry of contaminants. Likewise, a well-formed stoma is resistant to torsional stresses and accidental dislodgement. The results of these studies suggest that after scale-up to manufacturing, a Sharklet-micropatterned PG tube will accelerate stoma maturation reducing several common complications associated with poor or slow stoma formation (e.g., hypergranulation, skin breakdown and device dislodgement) in follow-up preclinical and clinical studies.

Conclusion

Here we demonstrated the Sharklet micropattern accelerates epithelial cell migration via apical contact guidance in a 2D modified scratch wound assay (4-fold increase, $p = 0.0105$) and an *in vitro* stoma formation model developed using 3D cell culture technology (50% increase, $p < 0.0001$) when compared to smooth controls. This acceleration of apically-guided epithelial cell migration indicates that the Sharklet micropattern has the potential to accelerate stoma tract maturation and thus reduce skin-related complications associated with PG tube placement. Follow-on preclinical studies will be initiated in a porcine model to evaluate the potential of this novel technology to enhance stoma formation *in vivo* and improve the implementation of this widely-used medical device.

ORCID iDs

Tyler J D'Ovidio https://orcid.org/0000-0002-3795-1833
Duncan Davis-Hall https://orcid.org/0000-0003-1280-8018
Chelsea M Magin https://orcid.org/0000-0002-6988-8584

References

[1] Gauderer M W L, Ponsky J L and Izant R J Jr 1980 Gastrostomy without laparotomy: a percutaneous endoscopic technique *Journal of Pediatric Surgery* **15** 872–5
[2] Kurien M, McAlindon M E, Westaby D and Sanders D S 2010 Percutaneous endoscopic gastrostomy (PEG) feeding *Brit. Med. J.* **7** 340
[3] Franken J, Mauritz F A, Suksamanapun N, Hulsker C C C, van der Zee D C and van Herwaarden-Lindeboom M Y A 2015 Efficacy and adverse events of laparoscopic gastrostomy placement in children: results of a large cohort study *Surg. Endosc.* **29** 1545–52.
[4] Milanchi S and Wilson M T 2008 Malposition of percutaneous endoscopic-guided gastrostomy: guideline and management *Journal of Minimal Access Surgery* **4** 1–4
[5] Winter G D 1974 Transcutaneous implants: reactions of the skin-implant interface *J. Biomed. Mater. Res.* **8** 99–113
[6] Göthberg G and Björnsson S 2015 One-Step Insertion of low-profile gastrostomy in pediatric patients vs pull percutaneous endoscopic gastrostomy *Journal of Parenteral and Enteral Nutrition.* **40** 423–30.

[7] Foutch P, Talbert G, Gaines J and Sanowski R 1989 The gastrostomy button: a prospective assessment of safety, success, and spectrum of use *Gastrointestional Endoscopy.* **35** 41–4
[8] Curtis A S G and Varde M 1964 Control of cell behavior: topological factors *Journal of the National Cancer Institute.* **33** 15–26
[9] Clement A L and Pins G D 2016 10 - Engineering the tissue–wound interface: harnessing topography to direct wound healing *Wound Healing Biomaterials* ed M S Ågren (Cambridge, United Kingdom: Woodhead Publishing) p 253–75
[10] Odland G F 1950 The morphology of the attachment between the dermis and the epidermis *Anatomical Rec.* **108** 399–413
[11] Magin C M *et al* 2016 Evaluation of a bilayered, micropatterned hydrogel dressing for full-thickness wound healing *Exp. Biol. Med. (Maywood)* **241** 986–95.
[12] Bush K A and Pins G D 2012 Development of microfabricated dermal epidermal regenerative matrices to evaluate the role of cellular microenvironments on epidermal morphogenesis *Tissue Eng. Part A* **18** 2343–53
[13] Dalton B A *et al* 2001 Modulation of epithelial tissue and cell migration by microgrooves *J. Biomed. Mater. Res.* **56** 195–207
[14] Clement A L, Moutinho T J and Pins G D 2013 Micropatterned dermal–epidermal regeneration matrices create functional niches that enhance epidermal morphogenesis *Acta Biomater.* **9** 9474–84
[15] Chehroudi B and Brunette D M 2002 Subcutaneous microfabricated surfaces inhibit epithelial recession and promote long-term survival of percutaneous implants *Biomaterials* **23** 229–37
[16] Feinberg A W, Schumacher J F and Brennan A B 2009 Engineering high-density endothelial cell monolayers on soft substrates *Acta Biomater.* **5** 2013–24.
[17] Magin C M, May R M, Drinker M C, Cuevas K H, Brennan A B and Reddy S T 2015 Micropatterned protective membranes inhibit lens epithelial cell migration in posterior capsule opacification model *Translational Vision Science and Techology.* **4** 1–8
[18] Underwood R A *et al* 2011 Quantifying the effect of pore size and surface treatment on epidermal incorporation into percutaneously implanted sphere-templated porous biomaterials in mice *J. Biomed. Mater. Res. Part A* **98A** 499–508
[19] Marmaras A *et al* 2012 Topography-mediated apical guidance in epidermal wound healing *Soft Matter.* **8** 6922–30
[20] Magin C M *et al* 2016 Evaluation of a bilayered, micropatterned hydrogel dressing for full-thickness wound healing *Experimental Biology and Medicine.* **241** 986–95
[21] Magin C M, May R M, Drinker M C, Cuevas K H, Brennan A B and Reddy S T 2015 Micropatterned protective membranes inhibit lens epithelial cell migration in posterior capsule opacification model *Translational Vision Science & Technology.* **4** 9
[22] Blumenstein I, Shastri Y M and Stein J 2014 Gastroenteric tube feeding: techniques, problems and solutions *World Journal of Gastroenterology.* **20** 8505–24
[23] Lohsiriwat V 2013 Percutaneous endoscopic gastrostomy tube replacement: a simple procedure? *World Journal of Gastrointestinal Endoscopy.* **5** 14–8
[24] Rosenberger L H, Newhook T, Sawyer R G and Schirmer B D 2011 Late accidental dislodgement of the percutaneous endoscopic gastrostomy: an underestimated burden on patients and the healthcare system *Gastroenterology.* **140** S–1041
[25] Conlon S J, Janik T A, Janik J S, Hendrickson R J and Landholm A E 2004 Gastrostomy revision: incidence and indications *Journal of Pediatric Surgery.* **39** 1390–5
[26] O'Dowd M, Given M F and Lee M J 2004 New approaches to percutaneous gastrostomy *Semin. Intervent. Radiol.* **21** 191–7
[27] McClain S A *et al* 1996 Mesenchymal cell activation is the rate-limiting step of granulation tissue induction *The American Journal of Pathology.* **149** 1257–70
[28] Huttenlocher A and Horwitz A R 2011 Integrins in cell migration *Cold Spring Harb. Perspect. Biol.* **3** a005074
[29] Haisler W L, Timm D M, Gage J A, Tseng H, Killian T C and Souza G R 2013 Three-dimensional cell culturing by magnetic levitation *Nat. Protoc.* **8** 1940
[30] Tseng H *et al* 2015 A spheroid toxicity assay using magnetic 3D bioprinting and real-time mobile device-based imaging *Sci. Rep.* **5** 13987
[31] Tseng H *et al* 2014 A three-dimensional co-culture model of the aortic valve using magnetic levitation *Acta Biomater.* **10** 173–82
[32] Jaganathan H *et al* 2014 Three-dimensional *in vitro* co-culture model of breast tumor using magnetic levitation *Sci. Rep.* **4** 6468